Anal. Chem. **2008,** *80,* 5970–5975

Biomimetically Synthesized Silica–Carbon Nanofiber Architectures for the Development of Highly Stable Electrochemical Biosensor Systems

Vicky Vamvakaki, Maria Hatzimarinaki, and Nikos Chaniotakis*

Laboratory of Analytical Chemistry, Department of Chemistry, University of Crete Voutes, P.O. Box 2208, 71003, Iraklion Crete, Greece

Biomimetically synthesized silica and conductive activated carbon nanofibers (CNFs) are used in a synergistic manner for the development of a novel electrochemical biosensor system. Poly(L-lysine) templated silica grows and encapsulates the CNF-immobilized enzyme generating a highly stabilizing nanostructured environment for the underlying protein. Concurrently, CNFs provide both the required surface area for the high-capacity enzyme immobilization required in biosensors as well as direct electron transfer to the inner platinum transducer. As a result, this silica/nanofiber superstructure is an ideal architecture for the development of electrochemical biosensor systems that can withstand exposure to extreme operational conditions, such as high temperatures or the presence of proteases. Acetylcholine esterase is used as the model catalyst and with the aid of spectroscopic data it is shown that the observed high operational stability of the biosensor is due to the direct interaction of the protein with the silica backbone, as well as due to the nanostructured enzyme confinement.

Nanomaterials offer new directions in the design of novel, analytically useful, nanobiosensing systems.[1–3] Nanomaterials with at least one of their critical dimensions in the range of 100 nm display unique physical and chemical characteristics. These materials can now be used in order to improve the analytical performance of biosensors, aiding in their establishment as reliable analytical instruments.[4,5] It is well-known, that the most critical issues in the application of in vivo biosensor systems are the stability of the biological sensing element (protein, enzyme, peptide, etc.) and the efficient and facile signal mediation and transduction for improved sensitivity and elimination of interferences. Nanomaterials have high surface-to-volume ratios, unique catalytic activities, and high electron-transfer rates at relatively low overpotentials. These characteristics make them ideal platforms for the design of electrochemical biosensors. In addition, they can be activated, thus acting as immobilization surfaces improving the stability of the attached proteins. One of the most promising such materials is carbon nanostructures,[6–18] some of which have already been successfully used for the development of stable electrochemical biosensors. Among these nanostructures, carbon nanofibers (CNFs) possess two unique physicochemical characteristics very useful in biosensor design, that of high conductivity and large active surface area.[19] CNFs are cylindrical nanostructures composed of graphite layers stacked around an axis and can be produced in different variations giving distinct, well-organized nanostructures. The large surface area of carbon nanofibers can be precisely controlled by thermal treatment, or chemical oxidation, providing large loading capacities for biological molecule attachment.[20,21] Further modification of these groups allows for the selective immobilization and stabilization of biomolecules such as proteins, enzymes,[19,22] and DNA.[23] In addition,

* To whom correspondence should be addressed. E-mail: nchan@chemistry.uoc.gr. URL: www.analytical_chemistry.uoc.gr. Tel: +30 2810 545 018. Fax: +30 2810 545 165.

(1) Vo-Dinh, T.; Cullum, B. M.; Stokes, D. L. *Sens. Actuators, B* **2001**, *74*, 2–11.
(2) Haruyama, T. *Adv. Drug Delivery Rev.* **2003**, *55*, 393–401.
(3) Jain, K. K. *Expert Rev. Mol. Diagn.* **2003**, *3*, 153–161.
(4) Jianrong, C.; Yuqing, M.; Nongyue, H.; Xiaohua, W.; Sijao, L. *Biotechnol. Adv.* **2004**, *22*, 505–518.
(5) Vaseashta, A.; Dimova-Malinovska, D. *Sci. Technol. Adv. Mater.* **2005**, *6*, 312–318.
(6) Gavalas, V. G.; Chaniotakis, N. A. *Anal. Chim. Acta* **2000**, *404*, 67–73.
(7) Sotiropoulou, S.; Chaniotakis, N. A. *Anal. Chim. Acta* **2005**, *530*, 199–204.
(8) Sotiropoulou, S.; Gavalas, V.; Vamvakaki, V.; Chaniotakis, N. A. *Biosens. Bioelectron.* **2003**, *18*, 211–215.
(9) Gavalas, V. G.; Chaniotakis, N. A. *Anal. Chim. Acta* **2000**, *409*, 131–135.
(10) Nednoor, P.; Capaccio, M.; Gavalas, V. G.; Meier, M. S.; Anthony, J. E.; Bachas, L. G. *Bioconjugate Chem.* **2004**, *15*, 12–15.
(11) Chaniotakis, N. A. In *Nanomaterials for biosensors*; Kumar, C. S. S. R., Ed.; Wiley-VCH: Weinheim, 2007; Vol. 8, pp 101–122.
(12) Fan, J.; Yudasaka, M.; Miyawaki, J.; Ajima, K.; Murata, K.; Iijima, S. *J. Phys. Chem. B* **2006**, *110*, 1587–1591.
(13) Sotiropoulou, S.; Chaniotakis, N. A. *Anal. Bioanal. Chem.* **2003**, *375*, 103–105.
(14) Besteman, K.; Lee, J. O.; Wiertz, F. G. M.; Heering, H. A.; Dekker, C. *Nano Lett.* **2003**, *3*, 727–730.
(15) Boo, H.; Jeong, R. A.; Park, S.; Kim, K. S.; An, K. H.; Lee, Y. H.; Han, J. H.; Kim, H. C.; Chung, T. D. *Anal. Chem.* **2006**, *78*, 617–620.
(16) Joshi, P. P.; Merchant, S. A.; Wang, Y.; Schmidtke, D. W. *Anal. Chem.* **2005**, *77*, 3183–3188.
(17) Tang, X.; Bansaruntip, S.; Nakayama, N.; Yenilmez, E.; Chang, Y. I.; Wan, Q. *Nano Lett.* **2006**, *6*, 1632–1636.
(18) Wang, J.; Liu, G.; Jan, M. R. *J. Am. Chem. Soc.* **2004**, *126*, 3010–3011.
(19) Vamvakaki, V.; Tsagaraki, K.; Chaniotakis, N. *Anal. Chem.* **2006**, *78*, 5538–5542.
(20) Lakshminarayanan, P. V.; Toghiani, H.; Pittman Jr, C. U. *Carbon* **2004**, *42*, 2433–2442.
(21) Toebes, M. L.; van Heeswijk, J. M. P.; Bitter, J. H.; van Dillen, A. J.; de Jong, K. P. *Carbon* **2004**, *42*, 307–315.
(22) Baker, S. E.; Colavita, P. E.; Tse, K. Y.; Hamers, R. J. *Chem. Mater.* **2006**, *18*, 4415–4422.
(23) Baker, S. E.; Tse, K. Y.; Hindin, E.; Nichols, B. M.; Clare, T. L.; Hamers, R. J. *Chem. Mater.* **2005**, *17*, 4971–4978.

10.1021/ac800614j CCC: $40.75
Published on Web 07/02/2008

their high conductance allows the efficient and facile electron transfer to the electrode surface for the signal transduction.[24,25]

Even though adsorption or covalent immobilization of the protein onto the surface of the CNFs provides a significant stabilization effect, this is not sufficient for highly stable implantable biosensor systems. Since enzymes are not very stable outside their biological environment, such as the one found in biosensor sensing elements, they are prone to denaturation or inactivation by even very small changes in pH, temperature, or the presence of traces of organic solvents and detergents usually employed for the construction of a biosensor. Another very important, but usually not well studied, factor drastically influencing the biosensor stability is the presence of proteases, found in all analyte solutions. Finally, enzyme leaching from the sensor surface to the solution is another problem, causing signal drift, and decreasing of the biosensor sensitivity over time. All these parameters have a detrimental effect on the analytical characteristics of the biosensor, decreasing both the operational and storage stabilities of biosensors—effects that are very profound when these biosensors are deployed in harsh environments or in vivo.

Recently, silica biomimetic composites have proven to be an excellent matrix for the encapsulation and stabilization of enzymes. Based on the silica formation that takes place in nature,[26–28] biomimetic analogues have been studied for the bioinspired silica formation onto different templates. The biological or synthetic peptide-directed growth has been reported to provide a variety of silica architectures, depending on experimental conditions.[29–31] The encapsulation of enzymes such as catalase, horseradish peroxidase,[32] and butyrylcholin esterase[33] in R5 peptide mediated silica or of nitrobenzene nitroreductase[34] in polyethyleneimine templated silica haS been shown to enhance the enzyme stabilities significantly. In addition, the entrapment of glucose oxidase in silica, in the presence of carbon nanotubes, has been also shown to allow the direct electron transfer from the enzyme to the immobilization surface.[35]

In this study, we utilize the advantages of two different nanobiotechnologies, CNFs and biomimetically synthesized silica, for the development of a novel enzyme electrochemical biosensor system. Initially the enzyme is directly immobilized onto the CNFs, which also serve as the mediation and transduction platforms for signal monitoring. Subsequently, bioinspired poly(L-lysine) templated silica is grown under mild conditions around the enzyme. These steps result in decreasing both the thermal inactivation of the protein and the degradation from proteases found in the solution. As a proof of concept, the inherently unstable acetylcholine esterase from *Drosophila melanogaster* (*Dm*. AChE) is chosen. The enzyme interaction with the silica/nanofiber architecture is studied by attenuated total reflection Fourier transform (ATR-FT)-IR spectroscopy, while the operational stability was examined under continuous operation conditions, at elevated temperature, and in the presence of proteases.

EXPERIMENTAL SECTION

Reagents. HTE carbon nanofibers were purchased from Electrovac AG. Acetylcholine esterase from *Drosophila melanogaster* was kindly provided from Prof. Didier Fournier (University Paul Sabatier, Toulouse, France). Poly(L-lysine) hydrobromide (PLL, 20.000−30.000) was obtained from Fluka. Tetramethyl orthosilicate (TMOS 99+%) and acetylthiocholine chloride were purchased from Sigma.

All other reagents were of analytical grade. In all experiments, Nanopure water (~18 MΩ, EASYpure model D7033, Barnstead) was used.

Carbon Nanofiber Oxidation. CNF oxidation was carried out using concentrated H_2O_2. A 150-mg aliquot of CNF was dispersed in 150 mL of H_2O_2 solution (30% w/w). The dispersion was refluxed for 2 h, while irradiated with a UV lamp. The oxidized CNFs were rinsed with 10 mM NaOH solution and deionized water until neutral pH. The acid-treated CNFs were dried under vacuum at 100 °C overnight.

Preparation of Poly(L-lysine) Templated Silica and Silica/Nanofiber Composite. For each experiment, the precipitation mixture consisted of 100 μL of PLL solution (1.0 mM in Nanopure H_2O), 500 μL of 25 mM KH_2PO_4 buffer at pH 7.0 (for silica/PLL), or 500 μL of *Dm*. AChE phosphate solution (for silica/PLL/AChE), or 500 μL of immobilized *Dm*. AChE (on oxidized CNFs) phosphate solution (for silica/CNF/PLL/AChE), 300 μL of Nanopure water, and 100 μL of freshly prepared stock solution of silicic acid. The latter was prepared by hydrolysis of TMOS at a concentration of 1.0 M with 1.0 mM HCl solution. The mixtures were mixed in a vortex slowly, followed by centrifugation at 4000 rpm. The products obtained were washed twice with Nanopure water. Finally, the samples obtained were dried at room temperature overnight. Since the isoelectric point of AChE is 5.0, at the experimental conditions (pH = 7.0) the enzyme is negatively charged. The electrostatic interaction of the enzyme with the positively charged poly(L-lysine) template facilitates the entrapment of AChE during biosilification.

The schematic picture of encapsulation of *Dm*. AChE in the silica/nanofiber architecture is schematically presented in Figure 1.

Characterization of Silica/Nanofiber Composite. Scanning electron microscopy (SEM) images of the samples were obtained using a JEOL 7000 scanning microscope in SE mode without any sample pretreatment. The ATR-FT-IR spectra were recorded on a Thermo-Electron Nicolet 6700 FT-IR optical spectrometer with a DTGS KBr detector at a resolution of 2 cm^{-1}.

Electrochemical Measurements. The *Dm*. AChE loaded silica/nanofiber architecture was placed into platinum-backed electrode cells for evaluation. Electrochemical experiments were performed using a three-electrode system with a silver/silver

(24) Vamvakaki, V.; Chaniotakis, N. A. *Sens. Actuators, B* **2006**, *126*, 193–197.
(25) Wu, L.; Zhang, X.; Ju, H. *Anal. Chem.* **2007**, *79*, 453–458.
(26) Shimizu, K.; Cha, J.; Stucky, G. D.; Morse, D. E. *Proc. Natl. Acad. Sci. U. S. A.* **1998**, *95*, 6234–6238.
(27) Kroger, N.; Deutzmann, R.; Sumper, M. *Science* **1999**, *286*, 1129–1132.
(28) Cha, J. N.; Katsuhiko, K.; Zhou, Y.; Christiansen, S. C.; Chmelka, B. F.; Stucky, G. D.; Morse, D. E. *Proc. Natl. Acad. Sci. U. S. A.* **1999**, *96*, 361–365.
(29) Patwardhan, S. V.; Clarsonb, S. J.; Perrya, C. C. *Chem. Commun.* **2005**, 1113–1121.
(30) Belton, D. J.; Siddharth, V.; Patwardhan, C.; Perry, C. C. *J. Mater. Chem.* **2005**, *15*, 4629–4638.
(31) Jan, J. S.; Shantz, D. F. *Adv. Mater.* **2007**, *19*, 2951–2956.
(32) Naik, R. R.; Tomczak, M. M.; Luckarift, H. R.; Spain, J. C.; Stone, M. O. *Chem. Commun.* **2004**, 1684–1685.
(33) Luckarift, H. R.; Spain, J. C.; Naik, R. R.; Stone, M. O. *Nat. Biotechnol.* **2004**, *22*, 211–213.
(34) Berne, C.; Betancor, L.; Luckarift, H. R.; Spain, J. C. *Biomacromolecules* **2006**, *7*, 2631–2636.
(35) Ivnitski, D.; Artyushkova, K.; Rincn, R. A.; Atanassov, P.; Luckarift, H. R.; Johnson, G. R. *Small* **2008**, *4*, 357–364.

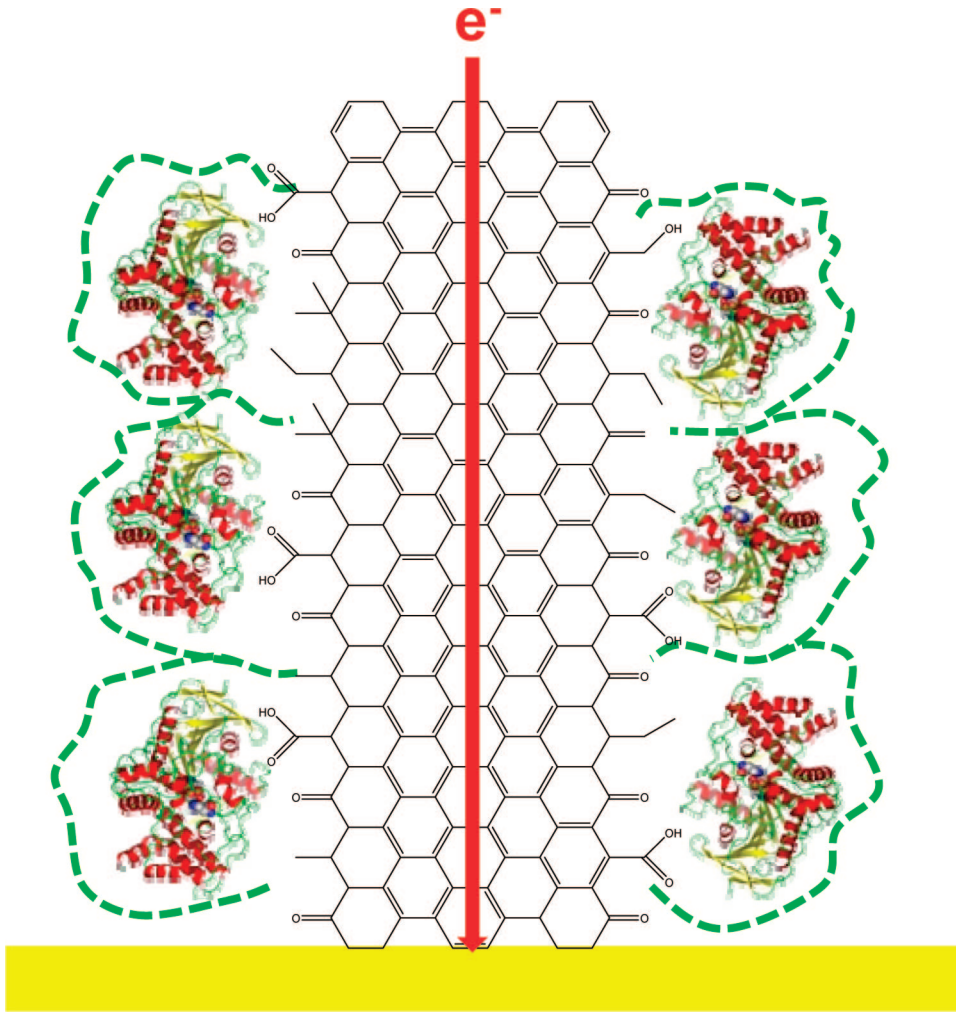

Figure 1. Schematic representation of the electrochemical silica/nanofiber-based biosensor setup. The dashed green line represents the shield provided by the biomimetically synthesized silica nanostructures. The electron transfer is achieved via the conductive CNFs, onto which the active enzyme is immobilized.

chloride double-junction reference electrode (model 90-02, ThermoOrion) and a 1-cm^2 platinum counter electrode (model 96-78-00, Orion). The potentiostat used was an Autolab PGSTAT 30 potentiostat/galvanostat equipped with a frequency response analyzer (Eco Chemie, The Netherlands). The sensitivity of the *Dm*. AChE biosensors was monitored amperometrically at the working potential of +300 mV versus Ag/AgCl electrode. In all experiments, the working solution was a phosphate buffer solution 25 mM, pH 7.0. Temperature control at 25.0 ± 0.1 °C was achieved using a circulating bath (model 362, PolyScience).

Stability Study. The *Dm*. AChE stability was examined by measuring the sensitivity of the AChE biosensors under continuous operation conditions applying a constant voltage of +300 mV versus Ag/AgCl. Enzyme thermal stability experiments were carried out by incubating the biosensors at 50 °C in the absence of substrate and then measuring the sensitivity of the corresponding biosensors at different times of incubation. The stability in the presence of proteases was determined by incubating the biosensors in 10 mg/mL Pronase for a specific time period and subsequently measuring the remaining sensitivity of the biosensors.

The free enzyme stability in each case was determined by the rate of acetylthiocholine chloride hydrolysis in potassium phosphate buffer (25 mM, pH 7.0) containing Ellman's reagent.[36] The reaction produces a yellow anion that can be detected photometrically at 412 nm using a UV−vis spectrophotometer (UNICAM 8625).

RESULTS AND DISCUSSION

Initially, the oxidized carbon nanofibers and silica/nanofiber architectures were characterized by SEM in order to determine their morphology and size distribution. The oxidized nanofibers have a mean diameter of 100 nm while their length is in the order of some tenths of micrometers (Figure 2A). The immobilization of the enzyme on the surface of the fibers and the further biosilification introduces silica particles along the fiber axis as shown in Figure 2B.

The efficient immobilization of *Dm*. AChE within the silica/nanofiber architecture was examined by ATR-FT-IR spectroscopy. The spectrum of poly(L-lysine) templated silica/nanofiber/AChE architecture was recorded and compared with that of the poly(L-lysine) templated silica nanocomposites and solid-state poly(L-lysine) and *Dm*. AChE. The characteristic peaks of the ATR-FT-

(36) Ellman, G. L.; Courtney, K. D. Jr.; Featherstone, R. M. *Biochem. Pharmacol.* **1961**, *7*, 88–95.

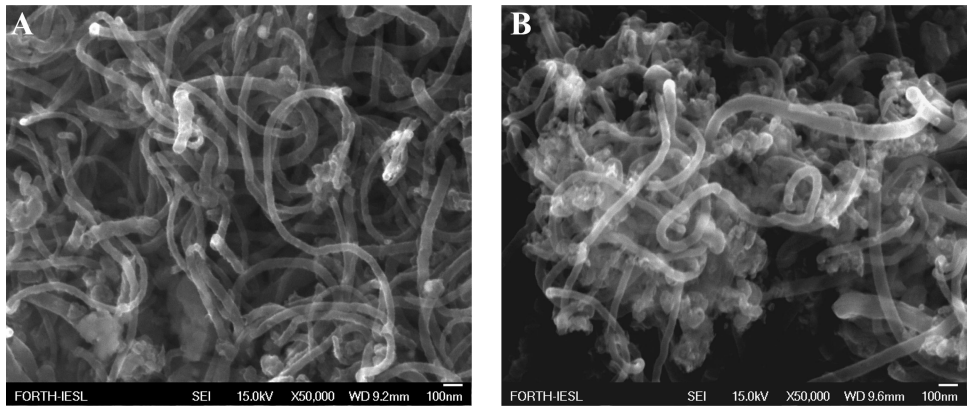

Figure 2. SEM images of (A) carbon nanofibers and (B) silica/nanofiber architecture.

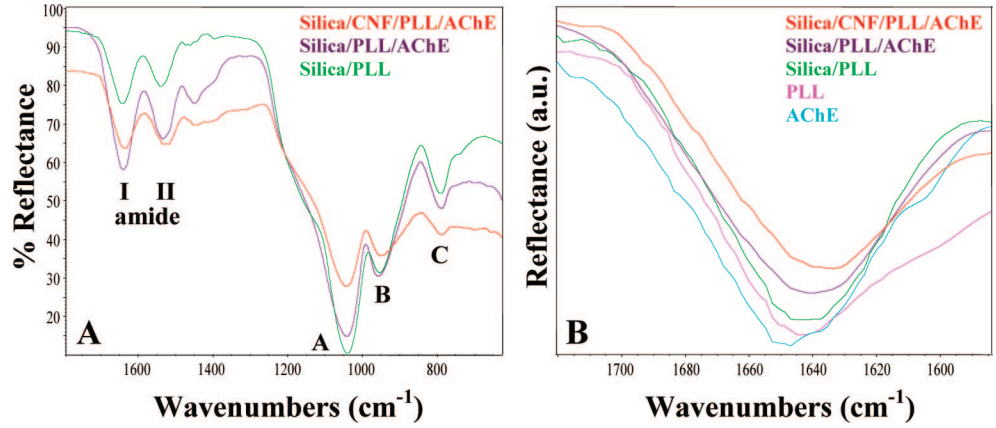

Figure 3. (A) ATR-FT-IR spectra of silica nanocomposites and (B) amide I band of *Dm.* AChE, PLL, and silica nanocomposites.

IR spectra are the amide I and II bands in the region of 1400−1700 cm^{-1} as well as silica peaks denoted A, B, and C in the region of 760−1300 cm^{-1} (Figure 3A). Amide I and II vibrations of a polypeptide backbone are the most studied peaks since they are very sensitive to changes of secondary conformations.[37,38] The shape of the amide I band (1620−1680 cm^{-1}) can provide information on the type and amount of the secondary structures.[39] At the same time, its line shape is not strongly influenced by side chains. As can be seen from Figure 3B, the amide I peak of intercalated poly(L-lysine) and *Dm.* AChE in the silica network are shifted in comparison to the amide I peak of the solid poly(L-lysine) and that of the *Dm.* AChE. These small but significant shifts observed are due to electrostatic or hydrophobic interactions of poly(L-lysine) and *Dm.* AChE with the silica matrix.[40,41] Poly(L-lysine) templated silica/nanofiber/AChE architecture displays the highest amide I shift toward lower wavenumbers compared to poly(L-lysine) and *Dm.* AChE confirming the interaction of poly(L-lysine) and protein residues with the silica network.

Silica peaks A and C arise from Si−O−Si asymmetrical and symmetrical stretching modes, respectively, while peak B is attributed to Si−O stretching mode either as silanol group (Si-OH) or as siloxane bridge ($Si-O^-$).[42−45] The maximum of the main silica peak (A), for all poly(L-lysine) templated silica nanocomposites, appears at lower wavenumbers (1043−1039 cm^{-1}) compared to the corresponding silica peak (1070−1100 cm^{-1}) of other sol−gel silica.[46,47] This shift can be atrributed to the presence of intercalated protein or poly(L-lysine) within the silica network, which affects the bond strength of neighboring Si−O−Si groups. Additionally, a relative increase of the intensity of band B compared to main band A is observed upon intercalation of *Dm.* AChE in the silica network. This increase is more pronounced for the poly(L-lysine) templated silica/nanofiber architecture. The latter can be attributed to a qualitative correlation between the intensity of band B and polypeptide amount. More nonbridging Si−O bonds are formed within the silica matrix and therefore involved in hydrogen bonds with poly(L-lysine) and *Dm.* AChE. Based on these data, it is evident that there is indeed enzyme encapsulation within the silica framework, as well as a close interaction of the surface functional groups of the protein with the silica/nanofiber sites.

The stabilizing effect of silica/nanofiber architecture to the enzyme AChE was examined by measuring the sensitivity of the

(37) Krimm, S.; Bandekar, J. *Adv. Protein Chem.* **1986**, *38*, 181–364.
(38) Bandekar, J. *Biochim. Biophys. Acta* **1992**, *1120*, 123–143.
(39) Barth, A.; Zscherp, C. *Q. Rev. Biophys.* **2002**, *35*, 369–430.
(40) Sotiropoulou, S.; Chaniotakis, N. A. *Biomaterials* **2005**, *26*, 6771–6779.
(41) Wu, S.; Ju, H.; Liu, Y. *Adv. Funct. Mater.* **2007**, *17*, 585–592.
(42) Almeida, R. M.; Guiton, T. A.; Pantano, C. G. *J. Non-Cryst. Solids* **1990**, *121*, 193–197.
(43) Perry, C. C.; Li, X.; Waters, D. N. *Spectrochim. Acta* **1991**, *47A*, 1487–1494.
(44) Innocenzi, P. *J. Non-Cryst. Solids* **2003**, *316*, 309–319.
(45) Fidalgo, A.; Cirimanna, R.; Ilharco, L. M.; Pagliaro, M. *Chem. Mater.* **2005**, *17*, 6686–6694.
(46) Bertoluzza, A.; Fagnano, C.; Morelli, M. A.; Gottardi, V.; Guglielmi, M. *J. Non-Cryst. Solids* **1982**, *48*, 117–128.
(47) Martinez, J. R.; Ruiz, F.; Vorobiev, Y. V.; Pérez-Robles, F.; González-Hernández, J. *J. Chem. Phys.* **1998**, *109*, 7511–7514.

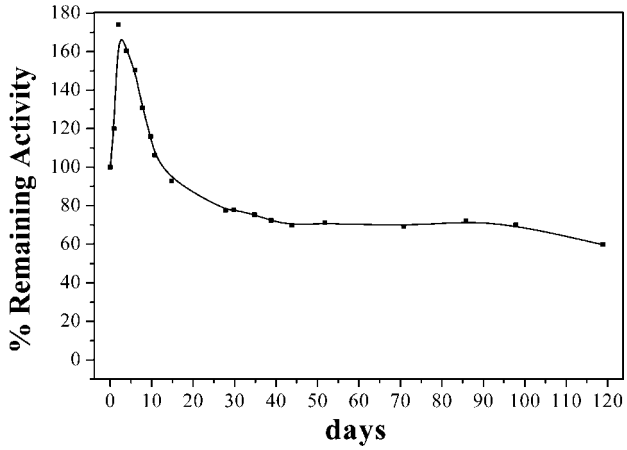

Figure 4. Stability under continuous polarization of AChE biosensor based on silica/nanofiber architecture (+300 mV, 25 °C).

corresponding biosensor under continuous polarization over time. Successive additions of acetylthiocholine lead to an increase of the anodic current, which is attributed to the oxidation of the enzyme's hydrolysis product thiocholine on the surface of the electrode. Reaction kinetics of the immobilized enzyme were determined from the substrate calibration curve presented in double inverse coordinates. The calculated apparent Michaelis constant K_M of the enzyme immobilized in the silica/nanofiber architecture was 0.34 mM, while the K_M value of both the free enzyme (determined by Ellman method[36]) and the enzyme entrapped in silica matrix are calculated 0.12 mM. This slight increase of the apparent K_M value in the case of the enzyme immobilized in the silica/nanofiber architecture can be attributed to the additional diffusion barrier or the structural changes in the enzyme conformation induced by carbon nanofibers. The sensitivity of the biosensor is directly related to the enzyme activity,[48] allowing the continuous monitoring of enzyme activity. The initial sensitivity of the silica/nanofiber/AChE biosensor is calculated to be 7.8 μA/mM. The response of biosensor is linear to acetylthiocholine concentrations from 0.04 to 0.3 mM. The response time of the biosensor is between 2 and 4 min, and the sensor-to-sensor reproducibility is less than 10% RSD ($n = 3$). As is shown in Figure 4, the biosensor has a remaining activity of 100% under continuous polarization for 13 days at 25 °C, poised at + 300 mV versus Ag/AgCl. The initial increase of the biosensor sensitivity is a well-known phenomenon in biosensor systems, attributed to changes of the enzyme's 3D structure inside the immobilization matrix upon rehydration.[49] Of considerable interest is the fact that the biosensor presented a remaining activity of 70% after 3.5 months of continuous polarization, while the free enzyme and the enzyme immobilized on carbon nanofibers (CNF/AChE) showed a considerable decrease of their activity to 50% after 25 and 4 days, respectively (data not shown). It is thus evident that the silica/nanofiber architecture provides an environment within which relatively unstable enzymes are highly stabilized based on continuous operational conditions experiments.

The same biosensor system was also examined for its ability to stabilize enzymes and protect them from denaturation under elevated temperatures. For this, the stability of the free and immobilized enzyme was examined under thermal stress of 50 °C. Figure 5A shows the stability of the free and silica stabilized enzyme, as calculated by the residual activity as a function of incubation time. The stability is expressed as the time at which the enzymatic activity is reduced to 50% (t_{50}) compared to the initial activity. The t_{50} of the free enzyme is measured to be only 4 min, while the immobilization of the enzyme on the nanofibers provides itself a 20-fold increase in the stabilization as the t_{50} increases to ~80 min, a result that is in agreement with previous reported nanofiber stabilization studies.[19] If now the nanofiber immobilized AChE is encapsulated via biosilification, the t_{50} of the system increases by a factor of 37, to 150 min. It is thus evident that enzyme immobilization on carbon nanofiber with subsequent silica nanocavity protection provides superior enzyme stabilization against thermal shock and protein denaturation.

Finally, the stability of the free and immobilized enzyme against external proteolysis was investigated. The resistance to proteolysis is a direct proof of the physical protection provided by the stabilizer to the protein structure.[50] Since proteases can be found in virtually any nonsterile solution, their effect on the biosensor element stability is a very important study needed to be performed in order to prove the ability of the system to be applied to real sample continuous analysis. As shown in Figure 5B, free enzyme loses its activity completely after only 1 h in Pronase solution, while the enzyme immobilized onto the nanofibers retains 37% of its initial activity after 2 h in the same solution. On the other hand, when the AChE enzyme is protected by silica through the biosilification procedure, its activity is virtually unaffected even after 12-h exposure to the Pronase. This last enzyme stability study shows also that the active protein is indeed encapsulated into the

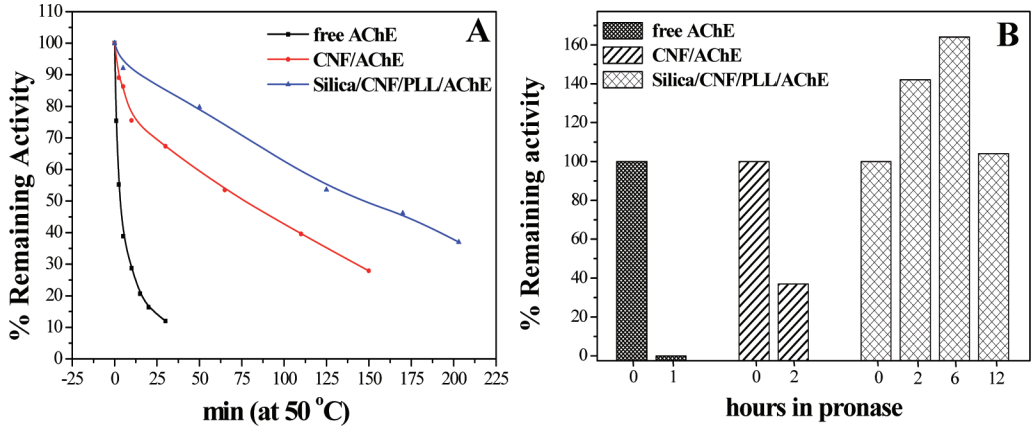

Figure 5. Stability study of free and immobilized AChE after incubation (A) at 50 °C and (B) in Pronase solution (10 mg/mL).

silica framework and not simply adsorbed onto its surface. It is thus clear that the silica nanocavities provide a physical barrier between the enzyme and the protease, decreasing the free energy of deactivation, while at the same time protecting the protein from protease attack.

CONCLUSSIONS

In this study, we have demonstrated that the synergistic effect of carbon nanofibers in combination with poly(L-lysine) templated silica provides ideal architectures for the design and development of highly stable biosensor systems. The unstable enzyme acetylcholine esterase was encapsulated in the silica/nanofiber architecture, and the corresponding biosensor has an operational lifetime of more than 3.5 months under continuous polarization. It is also shown that this silica/nanofiber architecture improves enzyme stabilization against thermal denaturation and complete protection from protease attack. The transduction efficiency of carbon nanofibers in combination with the enhanced stabilization of acetylcholine esterase encapsulated in poly(L-lysine) templated silica paves the way for a new class of biosensors that can find large-scale application in bioanalytical nanodevices.

(48) Rippeth, J. J.; Gibson, T. D.; Hart, J. P.; Hartley, I. C.; Nelson, G. *Analyst* **1997**, *122*, 1425–1430.
(49) Khan, G. F.; Wernet, W. *Anal. Chem.* **1997**, *69*, 2682–2687.
(50) Braxton, S.; Wells, J. A. *Biochemistry* **1992**, *31*, 7796–7801.

ACKNOWLEDGMENT

This work is being supported by the European Commission Programs "SANTS" (Contract 033254) and "NANOMYC" (Contract 036812). We thank Mrs. K. Tsagkaraki (microelectronics research group, FORTH, Crete, Greece) for the SEM images.

Received for review March 26, 2008. Accepted June 5, 2008.

AC800614J